ISSN 2635-1676, Nanobiotechnology Reports, 2022, Vol. 17, No. 2, pp. 193–201. © Pleiades Publishing, Ltd., 2022.

NANOBIOLOGY AND GENETICS, OMICS

Inactivation of Influenza Viruses with Heteropolyacids

F. I. Dalidchik[a], E. M. Balashov[a,*], O. V. Baklanova[b], E. A. Gushchina[b], N. M. Ivashkevich[c], E. I. Isaeva[b], S. A. Kovalevskiy[a], A. I. Kulak[c], O. A. Lopatina[b], I. T. Fedyakina[b], and M. V. Mezentseva[b]

[a] *Semenov Federal Research Center for Chemical Physics, Russian Academy of Sciences, Moscow, Russia*

[b] *Gamaleya National Research Center for Epidemiology and Microbiology, Ministry of Health of the Russian Federation, Moscow, Russia*

[c] *Institute of General and Inorganic Chemistry, National Academy of Sciences of Belarus, Minsk, Belarus*

**e-mail: embalashov@yandex.ru*

Received April 2, 2021; revised July 15, 2021; accepted July 20, 2021

Abstract—The antiviral activity of Keggin heteropolyacids (HPAs) against the human influenza A/California/07/09 (H1N1) pdm09 virus is studied in MDCK cell culture. Transmission electron microscopy reveals new features of the destruction of viral particles by HPAs. A proton-anion model that considers the main biochemical processes leading to the destruction of enveloped viruses: the depletion of membrane cholesterol by HPA anions, acidification of the M1 matrix protein by protons of the medium, and anion lysis of lipid membranes, is proposed. The Arrhenius dependences of the biological properties of HPAs on temperature are predicted. The general mechanism for the formation of high biological activity HPAs is described, which is underlined by the anion depletion of cholesterol in bilipid membranes, a new effect in the biochemistry of polyoxometalates.

DOI: 10.1134/S2635167622020070

INTRODUCTION

Influenza and other viral infections threaten human health. This threat is acutely manifested by the COVID-19 pandemic. There are concerns that the suppression of this infection will be hampered by the synergistic interaction of SARS-CoV-2 viruses and seasonal influenza [1, 2].

Due to virus mutations, the world is constantly in danger of nullifying the capabilities of all currently existing antiviral agents, which forces fundamental research aimed at elucidating the molecular nature of the biological activity of antiviral drugs and creating rapidly modified vaccines and drugs on this basis. One of the current directions of these works involves the use of polyoxometalates (POMs) [3–6].

POMs, known for a long time as effective catalysts, are intensively studied today as new promising nanomaterials, the range of possible applications of which extends from nanophysics and nanochemistry to nanobiology and nanomedicine [7–10]. In the last decade, the biological properties of POMs (antiviral, antibacterial, and anticancer [3–6]) have been supplemented by examples of the creation of new drugs based on them, promising for the treatment of Alzheimer's disease, hepatitis, asthma, and a number of new dangerous viral infections [10–12]. The antiviral activity of Keggin heteropolyacids (HPAs) has been established for many enveloped viruses [3–6, 10–20], including SARS-CoV-1 and MERS-CoV coronaviruses, which are genetic precursors of the SARS-Cov-2 virus [21, 22]. The first positive results of testing HPAs as effective inactivators of the SARS-Cov-2 virus were reported in [23].

High therapeutic indicators are usually achieved only with the careful selection of POMs and their corresponding biological targets. The causes for the high selectivity of POMs, which hinders the development of broad-spectrum therapeutic agents, as well as the very nature of the total high biological activity of POMs, remain unknown.

The aim of this work is to identify the main features of the concentration dependences of the biological activity of HPAs using the example of human influenza virus A(H1N1) (California/07/09 H1N1) and formulate a molecular biochemical model sufficient to describe the inactivation of influenza viruses by POM compounds at medium and high concentrations.

According to the proposed model, the processes of the destruction of cell membranes (CMs) and viral membranes by heteropolyacids begin with the depletion of membrane cholesterol by multiply charged anions, leading to the formation of through holes in the membranes, i.e., nanopores, which play the role of additional (lipid) ion channels. Depending on the HPA concentration, lipid composition of the membranes, temperature, and acidity of the medium, these nanodefects can either leak or, increasing in size, lead to the destruction (in some cases, to the collapse) of

bilipid membranes (BLMs). The processes of cell destruction and death under the influence of HPAs determine the toxicity of these compounds. In viral particles (VPs), the destruction of membranes is preceded by the processes of acidification (destruction) of the M1-matrix protein by protons of the medium. The destruction of this protein triggers two new processes leading to VP inactivation. One is associated with the removal of surface glycoproteins, the distal ends of which in native VPs are anchored in the M1 protein. The second process is the loss of functionally important properties by the matrix protein. At rather high HPA concentrations, the processes of anion etching of the edges of lipid ion channels can be effective simultaneously with the destruction of the M1 protein. These processes quickly transform nanopores into through microholes, through which proteins dissolved by protons flow out. Then etching of through defects in BLMs in some cases leads to the lysis of these structures. The proton-anion model provides a simple explanation of available experimental data on the destruction of viral particles by HPAs, predicts the temperature (Arrhenius) dependences of the biological properties of HPAs, and reveals the nature of the total high biological activity of POMs, linking it with a new effect for POM biochemistry, i.e., the depletion (up to 50%) of membrane cholesterol by multiply charged anions [24].

EXPERIMENTAL

Materials

Heteropolyacids. Vanadium-containing Keggin HPAs, $H_4PMo_{11}VO_{40}$, $H_5PMo_{10}V_2O_{40}$, and $H_4PW_{11}VO_{40}$, synthesized at the Institute of General and Inorganic Chemistry, National Academy of Sciences of Belarus, Minsk, were used.[1]

Viruses. The antiviral properties of the selected HPAs were studied using the example of the pandemic virus A/California/07/09, which was obtained from the State Collection of Viruses at the Gamaleya National Research Center for Epidemiology and Microbiology, Ministry of Health of the Russian Federation. The virus was cultured in the allantoic cavity of 9- and 10-day-old chicken embryos (48 h, 37°C). The infectious (IA) and hemagglutinating (HA) activities of viruses were determined by methods recommended by WHO [25].

Cell cultures. Canine kidney cells (MDCK) from the collection of cell cultures at the Gamaleya National Research Center for Epidemiology and Microbiology, Ministry of Health of the Russian Federation, were used. The cells were cultivated in MEM Eagle medium with a double set of amino acids, 5% fetal bovine serum (HyClone, United States), 10 mM glutamine, and 4% gentamicin.

[1] Vanadium-free analogs of these acids were studied in [20].

Methods

Determination of the cytotoxic effect of HPAs in MDCK cell culture. MDCK cells were introduced into 96-well plates at a concentration of 10000 cells/well in MEM Eagle medium (Institute of Poliomyelitis and Viral Encephalitis, Russian Academy of Medical Sciences) supplemented with 5% fetal bovine serum (HyClone), 10 mM glutamine and antibiotics and cultured for 72 h. Then after washing the cell culture twice with the serum-free MEM Eagle medium, aqueous solutions of HPAs prepared in advance in a supporting medium were introduced into the wells, starting from a dilution of 1 : 10 to a dilution of 1 : 5120. Each dilution was tested in four parallel wells. Further, the cells were incubated with the test substances for 72 h in a CO_2 incubator at a temperature of 37°C, after which the culture medium was removed and 100 μL of supporting medium and 20 μL of MTS solution (Promega, no. G3581) were added to each well. After incubation for 3 h at 37°C, the optical density was determined at a wavelength of 492 nm and a reference wavelength of 620 nm using a BIO-RAD plate spectrophotometer. The concentration of the test substance, which reduces the value of the optical density by 50% compared with the cell control, was taken as a 50% cytotoxic dose (CC_{50}).

The antiviral activity of the tested substances was considered by reducing the infectious titer of the influenza virus in MDCK cells by the cytopathic effect (CPE) and in the hemagglutination reaction (HAR).

MDCK cell culture was preliminarily prepared in the same way as in the experiments to determine the cytotoxic effect of HPAs. Before infection with the virus, the MDCK cells were washed twice with serum-free MEM Eagle medium and the studied substances were added at the required concentration in 100 μL of supporting medium and incubated for 1 h at 37°C. Then, 100 μL of preliminarily prepared 10-fold dilutions of the virus in MEM Eagle medium with the addition of trypsin (TPCK treated, Sigma) at a concentration of 2 μg/mL were added and incubated for 72 h in a CO_2 incubator at 37°C. The virus and cell controls were cultured in the same medium. The results were recorded according to CPE and in HAR. The hemagglutinating activity of the viruses was determined by HAR following the generally accepted method with 0.5% chicken erythrocytes. The pH of the medium after the addition of HPAs (100 μM) was 6.5.

The virucidal activity of the HPAs was determined by the results of their direct effect on influenza A/California/07/09(H1N1) pdm09 VPs. To do this, a virus suspension at a working dilution of 0.1 $TCID_{50}$ was added to 0.5 mL of a solution of tested HPAs of various concentrations (from 25 to 250 μM). In a control tube, 0.5 mL of MEM Eagle medium was added to 0.5 mL of the viral suspension. All prepared mixtures were incubated at a temperature of 26°C for 1 h. Then the

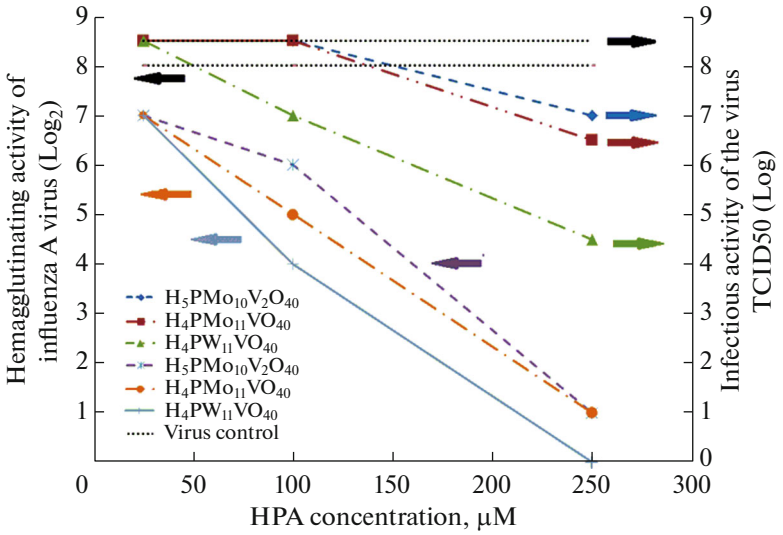

Fig. 1. Antiviral activity of HPAs against A/California/07/09 (H1N1) pdm09 virus reproduced in MDCK cell culture.

hemagglutination titer of each sample was determined in HAR. After 72 h, the infectious titer of the virus was determined in MDCK cell culture in control and experimental samples.

Electron microscopy (EM) of cells and viruses. The effect of HPAs on the structure of influenza virus A/California/07/09(H1N1) pdm09 in MDCK cell culture was studied by the method of ultrathin sections. The MDCK cells were cultured in 24-well plates using MEM Eagle medium with a double set of amino acids. After the formation of a single layer of cells, 100 μL of the medium with HPAs was added. After 2 h of incubation at 37°C, the cell single layer was infected with influenza virus A/California/07/09(H1N1) pdm09 at a dose of 0.1 TCID 50/cell. The cells were cultured under conditions of a CO_2 thermostat at 37°C for 24 h, then centrifuged, and the resulting deposit was fixed in a 2.5% solution of glutaraldehyde in 0.15-M phosphate buffer. The cell deposit was washed with phosphate buffer, fixed again with a 1% aqueous solution of OsO_4, successively desiccated in a series of alcohols, and dehydrated with propylene oxide. Impregnation and mounting of the deposit were carried out in EPON mixtures. Ultrathin sections were obtained on an LKB Broma ultratome, which were counterstained with a 5% solution of uranyl acetate and lead citrate.

The effect of HPAs on the morphology of influenza virions was studied by the method of negative contrast. A suspension containing influenza viruses A/California/07/09 at a concentration of 5.5 lgTCID50/mL was mixed in a ratio of 1 : 1 with aqueous HPA solutions. The concentration of HPAs was 100 μM. The mixture was incubated for 1 h at 25°C. The VP suspension treated with HPA samples was applied to a galvanic grid with a formvar substrate, dried for 30 min, and counterstained with a 1% aqueous solution of uranyl acetate. The samples were studied on a JEOL 100XC transmission electron microscope.

RESULTS

The toxic and antiviral effects of the studied HPAs are characterized by the results presented in Figs. 1–5 and in Tables 1, 2.

In analyzing the concentration dependences of the antiviral activity of the tested HPAs given in Table 2 and in Fig. 1, two features can be noted. The first one is the absence of the antiviral activity of all HPAs under the preliminary incubation of cells in nutrient media with a low acid content (12.5 μM). The decrease in the IA, which depends on the elemental composition of the HPAs, becomes rather large (0.5–3.0 $TCID_{50}$ Lg) only at concentrations of about CC_{50}. The cause for this decrease can be associated either with the primary action of HPAs on cells (before they are infected), or with the subsequent action of HPAs on both cells and viruses simultaneously. The answer is not difficult to obtain if we consider the results of testing the virucidal activity of HPAs, shown in Fig. 1. According to these results, in the case of the direct effect of HPAs on viral particles, the decrease in IA becomes significant only at concentrations exceeding 25 μM. Therefore, the decrease in IA observed at a concentration of 25 μM under conditions of virus replication in cell culture (Table 2) is associated with the action of HPAs only on cells.

In Fig. 2, one can notice a second interesting feature of the HA and IA concentration dependences of viruses measured after direct exposure of the viruses to various HPAs. At low concentrations, rather large changes in HA are regularly observed here (a twofold decrease), but there are no changes in IA.

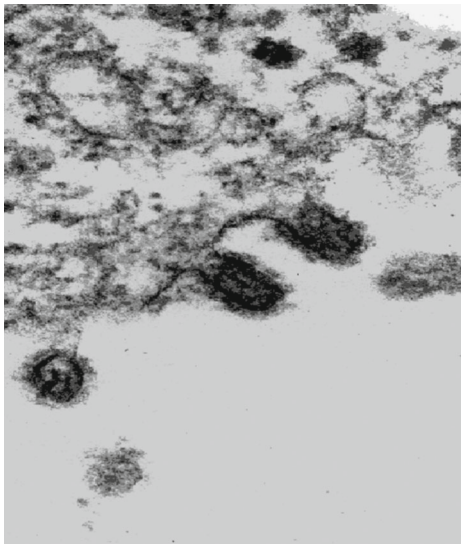

Fig. 2. Example of budding (oval) and detached (spherical) VPs near the surface of an intact MDCK cell infected with human influenza A/California/07/09(H1N1) pdm09 virus (control image).

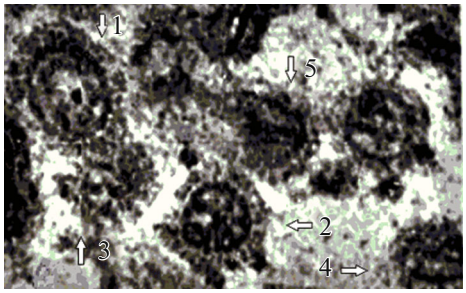

Fig. 4. Spherical VPs with defects of various types (initial stage of destruction): 1 is the intact particle, 2 is the particle with a small area of lost peplomers, 3 is the particle with fragmentary destroyed capsid and preserved area of peplomers, 4 is the particle with completely destroyed peplomer structure, 5 is the particle with a severely destroyed viral envelope and leaking proteins.

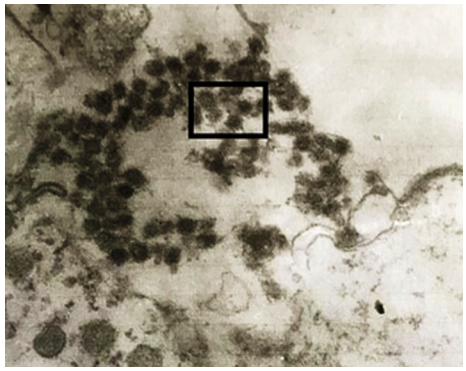

Fig. 3. Accumulation of spherical VPs at the edge of the rupture of the plasma membrane of an MDCK cell infected with influenza A/California/07/09 (H1N1) pdm09 virus ($H_4PMo_{10}VO_{40}$, 100 μM, 1 h). The frame highlights the area, an enlarged image of which is shown in Fig. 4.

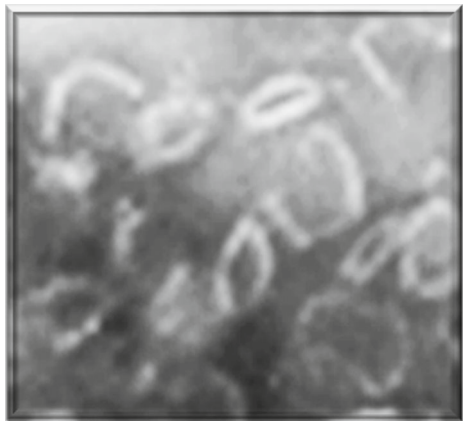

Fig. 5. Example of VP fragments with through microholes in envelopes and with destroyed proteins, which illustrates the small number of these defects on one envelope and an increase in the antiviral activity of HPAs with an increase in the anion charge described in [29] (A/California/07/09 (H1N1) pdm09, $H_5PMo_{10}V_2O_{40}$, 100 μM).

Morphological and Structural Characteristics of Cells and Viruses Before and After Exposure to HPAs

Examples of EM images demonstrating the morphological and structural features of MDCK cells and VPs of influenza A/California/07/09(H1N1) pdm09 before and after exposure to HPAs are shown in Figs. 2–5. The analysis of these (and many other generally similar) images leads to the conclusion that the destruction of CM, i.e., the process in this case determines the toxic properties of HPAs (Table 1), becomes significant at concentrations, at which virus envelopes can still be at the early stages of destruction. By analyzing the VP images given in Fig. 5, one can notice an interesting feature of surface defects such as through microholes (holes that are clearly visible on EM images); such defects are always few in number. There are no more than two or three of them on each envelope. Apparently, this is a common feature of through

Table 1. Cytotoxic effect of HPAs on MDCK cells

HPA	Cytotoxicity (CC_{50}), μM, incubation time 72 h
$H_5PMo_{10}V_2O_{40}$	25
$H_4PMo_{11}VO_{40}$	25
$H_4PW_{11}VO_{40}$	31

microholes that can be formed in BLMs under the influence of HPAs.[2]

The question concerning the mechanisms of the appearance and evolution of through holes in BLMs is of considerable interest; a large number of publications are devoted to it (for example, [23–25]). Below, we will propose an elementary model for the accelerated HPA-stimulated transformation of BLM nanopores into single microholes, the images of which, in addition to those shown in Fig. 5, are clearly visible in Fig. 2 of [22] and in Fig. 8 of [26].

DISCUSSION

Molecular Mechanisms of BLM Destruction by Heteropolyacids

At room temperature, the primary interactions of HPAs with viruses and cells may be considered as acts of the inelastic three-stage reflection of multiply charged anions from the corresponding BLMs [5, 26, 27]. According to these ideas, at the first stage, a vibrationally excited surface lipid-anion complex (LAC) is formed, which decomposes after relaxation. During decomposition, the new complex, which may include various membrane lipids, leaves the membrane. The probability of the removal of secondary complexes of a certain lipid composition W_{if} from the membrane depends on the temperature T and potential barriers V_{if} separating the areas of free movement of the removed (fth) complex and the areas of localization of its components in the decomposing (ith) complex:

$$W_{if} \sim \exp(-V_{if}/kT) \quad (1)$$

where k is the Boltzmann constant.

The higher the barrier values V_{if}, i.e., the activation energies of decomposition through certain channels, the higher the binding energy of this complex in BLMs. This leads to a fundamentally important conclusion about the depletion of weakly bound lipids of biological membranes by HPAs. Such lipids include cholesterol (in the case of defect-free membranes), as well as lipid molecules that form the edges of through surface defects from nanopores, the appearance of which can only be judged by indirect signs, for example, by an increase in the membrane permeability, to microholes that can be observed by EM methods.

Let us discuss the consequences of this conclusion, starting with the effect of cholesterol depletion, which was discovered in [24] by the method of the time-of-flight mass spectrometry of secondary ions when studying processes of the destruction of human embryonic fibroblast cells by solutions of silicomolybdic acid ($H_4SiMo_{12}O_{40}$, 10–100 μM, 300°C, 48 h).

[2] This conclusion can be reached by comparing Fig. 5 with Fig. 2 from [26], in which the collapse of a single liposome in an aqueous solution of Keggin HPAs was observed by fluorescence microscopy ($H_4SiW_{12}O_{40}$ and $H_3PW_{12}O_{40}$, 300 μM, 300°C, pH 7.5).

Table 2. Antiviral activity of HPAs against A/California/07/09 (H1N1) pdm09 virus in MDCK cell culture

HPA	HPA concentration, μM	Virus IA ($TCID_{50}$ Lg)
$H_5PMo_{10}V_2O_{40}$	25	9.5
	12.5	10.0
$H_4PMo_{11}VO_{40}$	25	9.0
	12.5	10.0
$H_4PW_{11}VO_{40}$	25	7.0
	12.5	10.0
Control	0	10.0

Cholesterol is a vital lipid that plays the role of a key regulator of all major biological properties of cell and virus membranes [28–31], including biomechanical properties such as fluidity and permeability, which increase with cholesterol depletion [32, 33]. Cellular cholesterol, synthesized in the endoplasmic reticulum, is contained mainly in the plasma membrane, more precisely, in "rafts", i.e., dense, strong, thickened, structurally well-organized surface clusters enriched in cholesterol and containing anchored proteins necessary for the vital function of cells [34–37]. The rafts are involved in many cellular and viral processes, playing a determinative role in all cases. When cholesterol is depleted (usually, methyl-β-cyclodextrin (MβCD) is used for this purpose [38, 39]), the rafts, losing lipid-binding molecules, are destroyed [40]. The consequences of such destruction, e.g., biological and medical, are well known today (for example, reviews [41, 42]).

The rafts contain proteins, some of which act as receptors necessary for the adsorption of VPs before the stage of their introduction into a cell. The assembly and budding of secondary (replication) VPs occurs on rafts [43, 44], so virus membranes are also significantly enriched in cholesterol, which is involved in almost all biochemical processes occurring at various stages of the life cycle. As a consequence, a decrease in cholesterol (regardless of the causes) in virus membranes is also accompanied by an adequate decrease in the infectious activity of VPs.

The decrease in cholesterol in virus membranes and the corresponding decrease in the IA of enveloped viruses under the influence of organic modulators (mainly MβCD) were previously investigated in many studies (for example, [44–50]). For HPAs, the role of cholesterol depletion in suppressing influenza IA is first demonstrated by the experimental results presented above.[3] The analysis of these results leads to

[3] It should be noted that the concentration dependences of IA, generally similar to those given for the virus A/California/07/09 (Fig. 1, Tables 2, 3), were also obtained by us for other strains of human influenza A viruses, such as A/Aichi/1/68, A/Perth/16/06, A/Brisbane/10/07, A/Brisbane/07/07, A/California/07/09, A/Penza/55/2008 and A/PR8/34 (unpublished data).

Table 3. Virucidal activity of HPAs against influenza A/California/07/09 (H1N1) pdm09

HPA	Concentration, μM	CR/HA, %	CI/IA, %
$H_4PW_{11}VO_{40}$	250	99.61	47.06
	100	93.75	17.65
	25	50	0
$H_4PMo_{11}VO_{40}$	250	99.22	23.53
	100	87.5	0
	25	50	0

the construction of a physically transparent model for the destruction of CMs and VPs by new, heteropolyacid, cholesterol modulators.

Threshold Effect under Inhibiting IA in Cell Culture

Let us consider, for example, the threshold effect, which is demonstrated by the results shown in Table 2. The absence of a decrease in IA at a concentration of 12.5 μM, which is not associated with the effect of anions directly on viruses, can be considered as an indication of the absence of a decrease in cholesterol in cell rafts. This is possible at rather low concentrations of HPAs, when the loss of raft cholesterol through the anion mechanism can be compensated by the processes of its intracellular restoration. At higher concentrations (but still in the absence of a direct effect of HPAs on viruses, as is the case of the HPA concentration of 25 μM), when processes of cholesterol depletion in cell rafts prevail over processes of its restoration, the rafts are partially destroyed, which is manifested by a decrease in IA, depending on the elemental composition of the anion. This dependence can, apparently, be attributed to the dependence of the depletion rate of cellular cholesterol on the elemental composition of HPAs.

It is clear that, at rather high HPA concentrations, CM destruction processes can proceed simultaneously with the destruction of rafts. Starting from the acts of the nucleation of small defects (apparently, from nanopores) and accelerating (see below), these processes quickly lead to the destruction (in some cases, to the rupturing) of CMs and, accordingly, to cell death, which determines the CC_{50} values. The selective nature of the depletion of marginal lipids in these processes is manifested by the dependences of the cytotoxicity of HPAs on the elemental composition of their anions. An example of CM rupture, on the edge of which partially destroyed VPs are adsorbed, is shown in Fig. 3.

Proton-Anion Model of Enveloped Virus Inactivation

Let us discuss the mechanisms of VP destruction. They can be judged by analyzing the EM images of VPs shown in Figs. 2–5, and using the information presented in Tables 1–3 and in Fig. 1. First of all, let us note that at concentrations of about CC_{50} and higher, all components of VPs, lipid and protein, external (peplomers) and internal, can be destroyed to a certain extent. Examples of complete or partial destruction of peplomers are clearly visible on the EM images. The destruction of the M1-matrix protein, which in its native state retains the distal regions of transmembrane glycoproteins and imparts strength and rigidity properties to the viral envelope, can be judged by a number of external signs. For example, by the appearance of particles of irregular (nonspherical) shape and particles with surface indentations and a few microholes (or breaks) with signs of leaking proteins. The formation of any of these defects reduces the IA of viruses to a certain extent. The extent of the decrease in the IA, as follows from the experimental results (Fig. 1, Table 2), significantly depends on the concentration of HPAs and on the chemical composition of their anions.

Let us consider the molecular mechanisms of the formation of various VP defects in more detail, starting with the process of the anion depletion of membrane cholesterol. We note that, according to formula (1), the rates of this depletion depend exponentially on temperature. Similar dependences can be expected for the biological properties of HPAs, if the latter are formed by secondary processes, the rates of which are limited by acts of cholesterol depletion.

The coefficient of the reduction (CR) of HA is defined in Table 3 by the ratio: $CR/HA = (1 - HA(C)/HA(0))\ 100\%$, where $HA(C)$ is the HA of viruses after exposure to a solution of HPAs of a given concentration C. $HA(0)$ is the HA value without the use of HPAs. The coefficient of inhibition (CI) of infectious activity (CI/IA) is determined by the same expression with the replacement of HA by IA, lg.

The processes of the destruction and rearrangement of surface proteins (transmembrane glycoproteins), proton channels (M2 proteins), and M1-matrix proteins can act as secondary processes that reduce the IA of viruses. Let us describe the mechanisms of these processes, focusing on the results of titration and EM studies. Given the data in Table 3, let us distinguish two stages of suppression of the infectious activity of VPs. The first corresponds to low concentrations of HPAs, at which a decrease in the titer of the HA is observed, but the titer of the IA remains unchanged. The second stage corresponds to higher concentrations of HPAs. Here, a symbate anion-dependent decrease in both titers is observed, and as the concentration increases, the decrease in the IA titers increasingly outpaces the decrease in HA titers. These features of the correlating titers of HA and IA can be explained if we take into account that the initial depletion of cholesterol in viral membranes increases their fluidity [32, 33], while, obviously, the strength of fix-

ation of the proximal regions of transmembrane glycoproteins decreases. As a result, it becomes possible to disrupt the native organization of the system of spikes, which can be manifested by an experimentally observed decrease in the adsorption capacity of VPs on erythrocytes. However, in general, the structure and properties of glycoproteins, as well as the structure of the M1 protein, in which the spikes are anchored, can remain unchanged with an increase in the fluidity of the viral membrane. In this case, the IA of particles can also remain unchanged. To remove spikes, i.e., to reduce the IA, which is observed at higher concentrations, the destruction (dissolution [51]) of the M1 protein is required. This is possible under the influence of protons in the medium penetrating the viral envelope through transmembrane proton channels, protein, M2, and/or lipid channels. M2 proton channels are opened only in acidic media, when the pH < 5 [51]. In the experiments performed, the acidity of the medium was noticeably lower (pH ≈ 6.5). i.e., the penetration of protons through the viral membrane was most likely carried out through the lipid channels.[4]

The possibility of the formation of membrane nanopores (lipid ion channels) during the depletion of viral cholesterol has apparently not been previously discussed. This hypothesis is one of the conclusions of this work, the reliability of which is confirmed by the results of EM studies shown in Figs. 3, 4, as well as in Fig. 8 of [26]. Here, individual microholes are clearly visible, which could be formed during the etching of nanopores with anions. Let us describe a probable mechanism for the formation of such microholes. Let us distinguish two main stages in it. At the first stage, the possibility of the stochastic formation of multiple, but small and unstable hydrophilic nanopores appears as a result of an increase in membrane fluidity and, accordingly, an increased probability of large-scale density fluctuations [53–55]. Subsequent etching of the edges of these pores with HPA anions is carried out according to the mechanism of formation and decomposition of edge LACs. Since at each moment of time the probability of the formation of an edge complex is proportional to the size of the existing defect, L, the kinetics of BLM destruction under the action of anions should obviously be exponential:

$$L(t) \sim \exp(Kt/\tau), \quad (2)$$

where L is the characteristic size of the through hole; τ is the lifetime of the marginal LAC; K is the dimensionless constant that depends on the structure of the decomposing marginal LAC. According to (2), the processes of the transformation of nanodefects into microholes have the character of the fast dissolution (collapses) of BLMs.[5] Within this model, the experimentally observed small number of visible surface defects is a consequence of the high rate of nanohole etching (small times τ/K compared with the characteristic times of nanopore nucleation).

We note that detachment of the distal ends of transmembrane glycoproteins from the partially destroyed (dissolved) M1-matrix protein is an important process, but not the only one, leading to VP inactivation. Taking into account the well-known role of this protein in the life cycle of a virus [51], it should be expected that with an increase in the concentration of HPAs, the increasing destruction of M1, slightly reducing the already low level of HA, will increasingly destroy VPs, thus reducing the IA values. This is what is observed in the experiment (Table 3).

When evaluating the above results of studying the antiviral activity of HPAs in cell culture, it should be borne in mind that at rather high concentrations (on the order of or more than CC_{50}) in the case of enveloped viruses, the membranes of which are formed from plasmolytic membranes containing a large amount of cholesterol (for example, in the case of influenza A), VP destruction may be unlikely (compared with CM destruction). For enveloped viruses, the membranes of which are formed from intracellular, weaker membranes (containing a small amount of cholesterol), the destruction of VPs should be predominant. Examples of such PVs include hepatitis C [10, 11], Zika [12], and numerous coronaviruses, including the pandemic viruses SARS-CoV-1, MERS-CoV, and SARS-CoV-2 [21, 22].

CONCLUSIONS

Let us note the significance of the conclusion made in the work on the destruction of cholesterol rafts by multiply charged HPA anions. Considering the important, often determinative role of these surface structures in many cellular and viral processes [34–37], it can be assumed that the depletion of cholesterol in rafts is one of the main causes for the total high biological activity of HPAs and POMs.

Let us also note the possible importance of lipid ion channels in processes of coronavirus inactivation [56]. Since an increase in the membrane fluidity and a corresponding increase in the probability of the spontaneous formation of nanopores are possible not only under cholesterol depletion, but also with an increase in temperature, it should be expected that for the SARS-CoV-2 virus, the formation of lipid ion channels will be manifested by a pronounced acidic effect: accelerated death of viruses in a narrow temperature range (near the main phase transition, $T_0 \approx 30$°C [57]) in media with rather low pH values.

[4] Another, possibly additional mechanism for the penetration of protons through the membrane is associated with the dependence of the conductivity of the M2 channel on membrane cholesterol [52].

[5] The observation of collapse of single liposomes in HPA solutions was reported in [26].

FUNDING

The work was carried out within the State Task on the topic "Basic foundations for creating nanostructured systems of a new generation with unique operational electrical and magnetic properties" no. 0082-2018-0003 (registration number AAAA-A18-118012390045-2) and with financial support of the Russian Foundation for Basic Research (project no. 18-54-00004 Bel_a) and the Belarusian Foundation for Basic Research (agreement no. X18P-110).

REFERENCES

1. S. Azekawa, H. Namkoong, K. Mitamura, et al., IDCases **20**, e00775-1–3 (2020). https://doi.org/10.1016/j.idcr.2020.e00775
2. J. Stowe, E. Tessier, H. Zhao, et al., medRxiv (2020). https://doi.org/10.1101/2020.09.18.20189647
3. J. T. Rhule, C. L. Hill, D. A. Judd, et al., Chem. Rev. **98**, 327 (1998). https://doi.org/10.1021/cr960396q
4. B. Hasenknopf, Front. Biosci. **10**, 275 (2005). https://doi.org/10.2741/1527
5. A. Bijelic, M. Aureliano, and A. Rompel, Angew. Chem. Int. Ed. Engl. **58**, 2980 (2019). https://doi.org/10.1002/anie.201803868
6. T. Yamase, J. Mater. Chem. **15**, 4773 (2005). https://doi.org/10.1039/B504585A
7. F. I. Dalidchik, E. M. Balashov, B. A. Budanov, A. K. Gatin, M. V. Grishin, A. A. Kirsankin, S. A. Kovalevskii, N. N. Kolchenko, V. G. Slutskii, and B. R. Shub, Russ. J. Phys. Chem. B **4**, 896 (2010).
8. M. T. Pope, *Encyclopedia of Inorganic and Bioinorganic Chemistry,* 1st ed., Ed. by R. A. Scott (Wiley, Somerset, NJ, 2011).
9. D. L. Long, R. Tsunashima, and L. Cronin, Angew. Chem. Int. Ed. **49**, 1736 (2010). https://doi.org/10.1002/anie.200902483
10. M. T. Pope, M. Sadakane, and U. Kortz, Eur. J. Inorg. Chem. **3–4**, 340 (2019). https://doi.org/10.1002/ejic.201801543
11. Y. Qi, L. Han, Y. Qi, et al., Antivir. Res. **179**, 104813 (2020). https://doi.org/10.1016/j.antiviral.2020.104813
12. R. Francese, A. Civra, M. Ritta, et al., Antivir. Res. **163**, 29 (2019). https://doi.org/10.1016/j.antiviral.2019.01.005
13. O. A. Lopatina, I. A. Suetina, M. V. Mezentseva, L. I. Russu, S. A. Kovalevskiy, E. M. Balashov, S. A. Ulasevich, A. I. Kulak, D. A. Kulemin, N. M. Ivashkevich and F. I. Dalidchik, Russ. J. Phys. Chem. B **14**, 81 (2020).
14. S. Shigeta, Drugs R D. **2**, 153 (1999). https://doi.org/10.2165/00126839-199902030-00001
15. S. Shigeta, Antivir. Chem. Chemother. **12** (Suppl. 1), 179 (2001).
16. S. Shigeta and T. Yamase, Antivir. Chem. Chemother. **16**, 23 (2005). https://doi.org/10.1177/095632020501600103
17. S. Shigeta, S. Mori, J. Watanabe, et al., Antivir. Chem. Chemother. **7**, 346 (1996).
18. S. Shigeta, S. Mori, J. Watanabe, et al., Antimicrob. Agents Chemother. **41**, 1423 (1997). https://doi.org/10.1128/AAC.41.7.1423
19. S. Shigeta, S. Mori, T. Yamase, et al., Biomed. Pharmacother. **60**, 211 (2006). https://doi.org/10.1016/j.biopha.2006.03.009
20. O. A. Lopatina, E. I. Isaeva, I. A. Suetina, et al., Nanotekhnol.: Razrab., Primen.–XXI Vek **8** (2), 14 (2016).
21. F.-Y. Chang, H.-C. Chen, P.-J. Chen, et al., J. Biomed. Sci. **27**, 1 (2020). https://doi.org/10.1186/s12929-020-00663-w
22. Di E. Maria, A. Latini, P. Borgiani, and G. Novelli, Human Genomics **14**, 1 (2020). https://doi.org/10.1186/s40246-020-00280-6
23. K. Dan, K. Fujinami, and H. Sumitomo, Appl. Sci. **10**, 8246 (2020). https://doi.org/10.3390/app10228246
24. S. A. Kovalevskiy, A. A. Gulin, O. A. Lopatina, A. A. Vasin, M. V. Mezentseva, E. M. Balashov, D. A. Kulemin, A. I. Kulak, and F. I. Dalidchik, Nanotechnol. Russ. **14**, 481 (2019). https://doi.org/10.1134/S1995078019050082
25. R. U. Khabriev, *Guidelines for the Experimental (Preclinical) Study of New Pharmacological Substances* (Meditsina, Moscow, 2005) [in Russian].
26. D. Kobayashi, Y. Ouchi, M. Sadakane, et al., Chem. Lett. **46**, 533 (2017). https://doi.org/10.1246/cl.161172
27. A. Sakamoto, K. Unoura, and H. Nabika, J. Phys. Chem. C **122**, 1404 (2018). https://doi.org/10.1021/acs.jpcc.7b11251
28. F. R. Maxfield and G. van Meer, Curr. Opin. Cell Biol. **22**, 422 (2010). https://doi.org/10.1016/j.ceb.2010.05.004
29. S. Chakraborty, M. Doktorova, T. R. Molugu, et al., Proc. Natl. Acad. Sci. U. S. A. **202004807**, 1 (2020). https://doi.org/10.1073/pnas.2004807117
30. de Oliveira and L. Andrade, Biomed. Spectrosc. Imaging **5**, S101 (2016). https://doi.org/10.3233/bsi-160157
31. N. S. Heaton and G. Randall, Trends Microbiol. **19**, 368 (2011). https://doi.org/10.1016/j.tim.2011.03.007
32. R. A. Cooper, J. Supramol. Struct. **8**, 413 (1978). https://doi.org/10.1002/jss.400080404
33. F. Mollinedo, Front. Oncol. **2**, 140 (2012). https://doi.org/10.3389/fonc.2012.00140
34. D. A. Brown and E. London, Ann. Rev. Cell Dev. Biol. **14**, 111 (1998). https://doi.org/10.1146/annurev.cellbio.14.1.111
35. S. S. Braga, Biomolecules **9**, 801 (2019). https://doi.org/10.3390/biom9120801
36. G. Crini, Chem. Rev. **114**, 10940 (2014). https://doi.org/10.1021/cr500081p
37. A. E. Shristian, M. P. Haynes, M. C. Phillips, and G. H. Rothblat, J. Lipid Res. **38**, 2264 (1997).
38. A. Biswas, P. Kashyap, S. Datta, et al., Biophys. J. **116**, 1456 (2019). https://doi.org/10.1016/j.bpj.2019.03.016

39. S. Barman and D. P. Nayak, J. Virology **81**, 12169 (2007). https://doi.org/10.1128/jvi.00835-07
40. M. R. Breen, M. Camps, F. Carvalho-Simoes, et al., PLoS One **7**, e34516 (2012). https://doi.org/10.1371/journal.pone.0034516
41. J. D. Greenlee, T. Subramanian, K. Liu, and M. R. King, Cancer Res. (2020). https://doi.org/10.1158/0008-5472.can-20-2199
42. S. Chen, H. He, H. Yang, et al., J. Med. Virol. **91**, 949 (2019). https://doi.org/10.1002/jmv.25414
43. N. Chazal and D. Gerlier, Microbiol. Mol. Biol. Rev. **67**, 226 (2003). https://doi.org/10.1128/MMBR.67.2.226-237.2003
44. K. S. Choi, H. Aizaki, and M. M. C. Lai, J. Virol. **79**, 9862 (2005). https://doi.org/10.1128/jvi.79.15.9862-9871.2005
45. T. Ruiz-Herrero and M. F. Hagan, Biophys. J. **108**, 585 (2015). https://doi.org/10.1016/j.bpj.2014.12.017
46. H. Guo, M. Huang, Q. Yuan, et al., PLoS One **12**, e0170123 (2017). https://doi.org/10.1371/journal.pone.0170123
47. A. Kerviel, A. Thomas, L. Chaloin, et al., Virus Res. **171**, 332 (2013). https://doi.org/10.1016/j.virusres.2012.08.014
48. Q. Yang, Q. Zhang, J. Tang, and W.-H. Feng, Virology **484**, 170 (2015). https://doi.org/10.1016/j.virol.2015.06.005
49. P. Danthi and M. Chow, J. Virol. **78**, 33 (2004). https://doi.org/10.1128/JVI.78.1.33-41.2004
50. T. Takahashi and T. Suzuki, Open Dermatol. J. **3**, 178 (2009). https://doi.org/0.2174/1874372200903010178
51. O. P. Zhirnov and A. A. Manykin, Vopr. Virusol. **3**, 41 (2014).
52. A. Martyna, B. Bahsoun, J. J. Madsen, et al., J. Phys. Chem. B **124**, 6738 (2020). https://doi.org/10.1021/acs.jpcb.0c03331
53. V. F. Antonov, E. Yu. Smirnova, and E. V. Shevchenko, *Lipid Membranes during Phase Transformations of Membrane Lipids* (Nauka, Moscow, 1992) [in Russian].
54. N. E. Bogatyreva, E. V. Shevchenko, E. V. Yakovenko, A. M. Chernysh, M. V. Rainov, and V. F. Antonov, Biophysics **43**, 47 (1998).
55. N. A. Corvalán, J. M. Kembro, P. D. Clop, and M. A. Perillo, Biochim. Biophys. Acta **1828**, 1754 (2013). https://doi.org/10.1016/j.bbamem.2013.03.019
56. Guo Xiling, Chen Yin, Wang Ling, et al., Sci. Rep. **11**, 2418 (2021).
57. J. Gallaher, K. Wodzińska, T. Heimburg, and M. Bier, Phys. Rev. E **81**, 061925 (2010). https://doi.org/10.1103/PhysRevE.81.061925

Translated by D. Novikova